Ligand Field Circular Dichroism and Magnetic Circular Dichroism Studies of Component B and Substrate Binding to the Hydroxylase Component of Methane Monooxygenase

Sabine Coates Pulver,[†] Wayne A. Froland,[‡,§] John D. Lipscomb,*[,‡] and Edward I. Solomon*[,†]

Contribution from the Department of Chemistry, Stanford University, Stanford, California 94305 and Department of Biochemistry, University of Minnesota, Minneapolis, Minnesota 55455

Received August 14, 1996[⊗]

Abstract: The soluble methane monooxygenase system (MMO), consisting of a hydroxylase (MMOH), a reductase, and component B (MMOB), catalyzes the NADH and O_2 dependent hydroxylation of methane and many other hydrocarbons. The binuclear non-heme ferrous active site cluster of the hydroxylase−component B (MMOH−MMOB) complex in the presence of substrate and small molecules has been studied using circular dichroism (CD) and magnetic circular dichroism (MCD) spectroscopies. CD studies reveal that addition of the alternative substrate, *trans*-1,2-dichloroethylene, or inhibitor, tetrachloroethylene, induces a conformational change in the active site pocket only in the presence of MMOB. Complementary MCD data indicate that this conformational change does not result in a direct change in the ligation of the iron atoms. Comparison of the CD/MCD data with the crystal structure of MMOH allows a tentative correlation between the perturbations observed and the iron atoms affected. The binding of MMOB to MMOH distorts the ligand field environment of one iron, while substrate binding in the presence of MMOB perturbs the other, therefore providing insight into the regulatory role of MMOB and into the participation of the two iron centers in the reaction. Anion binding to the MMOH−MMOB complex was also investigated. No spectral perturbation by small molecules ($K_B < 30\ M^{-1}$) in reduced MMOH and the MMOH−MMOB complex was observed, suggesting that the hydroxylase active site pocket is less electrophilic than other binuclear non-heme iron proteins, consistent with its role in charge donation to activate dioxygen.

Introduction

An oxygen-bridged binuclear non-heme iron active site has been found in a number of metalloproteins including the following: hemerythrin (Hr),[1,2] methane monooxygenase (MMO),[3−7] toluene monooxygenase (TMO),[8,9] ribonucleoside diphosphate reductase (RDPR),[10−13] acyl carrier protein Δ^9 desaturase (ACP Δ^9D),[14,15] the purple acid phosphatases (PAP),[16−19] rubrerythrin (Rb),[20,21] and nigerythrin.[22] Where the function is known, the binuclear iron center plays a variety of roles involving dioxygen.[7,23−29] In Hr it binds dioxygen reversibly, in RDPR it reacts with O_2 to generate a tyrosyl radical necessary for the reduction of ribonucleotides to deoxyribonucleotides, in MMO and TMO it activates dioxygen for the hydroxylation of methane and toluene, respectively, in ACP Δ^9D it activates O_2 leading to the insertion of a 9,10 *cis* double bond in the conversion of stearoyl-ACP to oleyl-ACP, and in the PAPs it is oxidized by O_2 resulting in reversible protein inactivation. It has been of general importance to understand

[†] Stanford University.
[‡] University of Minnesota.
[§] Current address: Department of Chemistry, University of California at Berkeley, Berkeley, California 94720.
[⊗] Abstract published in *Advance ACS Abstracts,* December 15, 1996.

(1) Wilkins, P. C.; Wilkins, R. G. *Coord. Chem. Rev.* **1987**, *79*, 195.
(2) Klotz, I. M.; Kurtz, D. M. *Acc. Chem. Res.* **1984**, *17*, 16.
(3) Lipscomb, J. D. *Annu. Rev. Microbiol.* **1994**, *48*, 371.
(4) Froland, W. A.; Andersson, K. K.; Lee, S.-K.; Liu, Y.; Lipscomb, J. D. In *Microbial Growth on C_1 Compounds*; Murrell, J. C., Kelly, D. P., Eds.; Intercept Ltd.: Andover, 1993; p 81.
(5) Fox, B. G.; Lipscomb, J. D. In *Biological Oxidation Systems*; Reddy, C. C., Hamilton, G. A., Madyastha, K. M., Eds.; Academic Press: New York, 1992; Vol. 1, p 367.
(6) Dalton, H. In *Advances in Applied Microbiology*; Umbreit, W. W., Ed.; Academic Press: New York, 1980; Vol. 26, p 71.
(7) Feig, A. L.; Lippard, S. J. *Chem. Rev.* **1994**, *94*, 759.
(8) Pikus, J. D.; Studts, J. M.; Achim, C.; Kauffmann, K. E.; Münck, E.; Steffan, R. J.; McClay, K.; Fox, B. G. *Biochemistry* **1996**, *35*, 9106.
(9) Newman, L. M.; Wackett, L. P. *Biochemistry* **1995**, *34*, 14066.
(10) Stubbe, J. *J. Biol. Chem.* **1990**, *265*, 5329.
(11) Nordlund, P.; Eklund, H. *J. Mol. Biol.* **1993**, *232*, 123.
(12) Reichard, P.; Ehrenberg, A. *Science* **1983**, *221*, 514.
(13) Sjöberg, B. M. In *Nucleic Acids and Molecular Biology*; Lilley, D. M. J., Ed.; Springer-Verlag: Berlin, 1995; Vol. 9, p 192.
(14) Fox, B. G.; Shanklin, J.; Somerville, C.; Münck, E. *Proc. Natl. Acad. Sci. U.S.A.* **1993**, *90*, 2486.
(15) Fox, B. G.; Shanklin, J.; Ai, J.; Loehr, T. M.; Sanders-Loehr, J. *Biochemistry* **1994**, *33*, 12776.
(16) Doi, K.; Antanaitis, C.; Aisen, P. In *Structure and Bonding*; Clarke, M. J., Goodenough, J. B., Ibers, J. A., Jorgensen, C. K., Mingos, D. M. P., Neilands, J. B., Palmer, G. A., Reinen, D., Sadler, P. J., Weiss, R., Williams, R. J. P., Eds.; Springer-Verlag: Heidelberg, 1988; Vol. 70, p 1.
(17) Vincent, J. B.; Averill, B. A. *FASEB J.* **1990**, *4*, 3009.
(18) Antanaitis, B. C.; Aisen, P. In *Frontiers in Bioinorganic Chemistry*; Xavier, A. V., Ed.; VCH: New York, 1986; p 481.
(19) Que, L.; Scarrow, R. C. In *Metal Clusters in Proteins*; Que, L., Ed.; American Chemical Society: Washington, DC, 1988; p 152.
(20) LeGall, B. G.; Prickril, B. C.; Moura, I.; Xavier, A. V. *Biochemistry* **1988**, *27*, 1636.
(21) deMare, F.; Kurtz, D. M.; Nordlund, P. *Nature Struct. Biol.* **1996**, *3*, 539.
(22) Pierik, A. J.; Wolbert, R. B. G.; Portier, G. L.; Verhagen, M. F. J. M.; Hagem, W. R. *Eur. J. Biochem.* **1993**, *212*, 237.
(23) Howard, J. B.; Rees, D. C. In *Advances in Protein Chemistry*; Anfinsen, C. B., Edsall, J. T., Eisenberg, D. S., Richards, F. M., Eds.; Academic Press Inc.: San Diego, 1991; Vol. 42, p 199.
(24) Que, L.; True, A. E. In *Progress in Inorganic Chemistry: Bioinorganic Chemistry*; Lippard, S. J., Ed.; John Wiley & Sons: New York, 1990; Vol. 38, p 97.
(25) Vincent, J. B.; Olivier-Lilley, G.; Averill, B. A. *Chem. Rev.* **1990**, *90*, 1447.
(26) Sanders-Loehr, J. In *Iron Carriers and Iron Proteins*; Loehr, T. M., Ed.; VCH Press: New York, 1989; p 373.
(27) Kurtz, D. M. *Chem. Rev.* **1990**, *90*, 585.
(28) Nordlund, P.; Eklund, H. *Curr. Opin. Struct. Biol.* **1995**, *5*, 758.
(29) Andersson, K. K.; Gräslund, A. *Adv. Inorg. Chem.* **1995**, *43*, 359.

S0002-7863(96)02854-5 CCC: $14.00

how differences in the binuclear non-heme iron center relate to these differences in dioxygen and substrate reactivities.

Methane monooxygenase catalyzes the NADH- and O_2-dependent hydroxylation of methane to methanol (eq 1).[6] This

$$\text{methane} + O_2 + \text{NADH} + H^+ \rightarrow NAD^+ + H_2O + \text{methanol} \quad (1)$$

reaction initiates the metabolic pathway that supplies the total carbon and energy needs of methanotrophic bacteria. In subsequent successive reactions, carbon originally derived from methane is oxidized enzymatically through formaldehyde and formic acid and finally to CO_2. Furthermore, although methane is the only substrate of MMO that can support rapid growth,[30] the enzyme system catalyzes the oxidation of many other saturated, unsaturated, linear, branched, and cyclic hydrocarbons, some at rates comparable to that of methane turnover.[6,31−36]

Soluble MMO isolated from *Methylosinus trichosporium* OB3b or *Methylococcus capsulatus* (Bath) is a three component system comprised of a 245-kDa hydroxylase (MMOH) with an $(\alpha, \beta, \gamma)_2$ subunit structure, a 40-kDa reductase containing both FAD and a [2Fe2S] cluster,[37,38] and a 15.8-kDa monomeric protein termed component B (MMOB) containing no metals or cofactors.[39,40] The reductase transfers reducing equivalents from NADH to the hydroxylase.[39,41] Component B plays several regulatory roles in catalysis, although it is not required for enzyme turnover.[39,42] The formation of complexes between the components has been demonstrated by a variety of kinetic, chemical, and spectroscopic techniques.[42−46] MMOB and the reductase appear to occupy specific binding sites on the α and β subunits, respectively, of MMOH. MMOH from *M. trichosporium* OB3b has been shown to contain two μ-hydroxo-bridged binuclear ferric [$Fe^{III}Fe^{III}$] clusters in the resting enzyme, which are positioned within the α subunits.[37,39,47−50] MMOH, and by implication the binuclear iron cluster, has been identified as the site of monooxygenase activity based on single turnover experiments with the fully reduced binuclear ferrous [$Fe^{II}Fe^{II}$] enzyme.[39]

Even though substrate binding and oxygen activation occurs at the hydroxylase, all three components of the MMO enzyme are required for efficient oxidation of substrate.[39] Steady-state kinetic studies on MMOH in the presence of MMOB have shown that MMOB has a dramatic effect on the rate of substrate oxidation.[43] Addition of MMOB to a system composed of NADH, O_2, reductase, and MMOH causes an increase in the initial rate of turnover by as much as 150-fold. This effect maximizes at a ratio of 1:1 for MMOB:MMOH active sites when the MMOH concentration is $>1\ \mu$M. It has recently been shown that this effect is due to the fact that MMOB increases both the rate of O_2 reaction with biferrous MMOH to yield the first transient intermediate in the catalytic cycle, compound P, and the rate of conversion of compound P to the second transient intermediate, compound Q which is described as a binuclear ferryl [$Fe^{IV}Fe^{IV}$]═O species.[51] MMOB also alters the redox potentials of the binuclear iron active site shifting the potential negative by 132 mV.[44−46] Lastly, MMOB also changes the product distribution of substrates more complex than methane.[42] It has been proposed that the effects on substrate oxidation rates, redox potentials, and product distribution are mediated by the formation of a stable complex between MMOH and MMOB.[39,42,43] Spectroscopic studies have further suggested that complex formation between MMOB and MMOH in some way affects the active site iron cluster.[37,43,52]

The three-dimensional structure of resting MMOH from *M. capsulatus* (Bath) has been determined by X-ray crystallography at 1.8 Å resolution.[53,54] A schematic of the crystal structure determined from a flash frozen crystal at −160 °C is shown in Figure 1A.[55] The Fe···Fe distance is 3.1 Å, and the iron atoms are bridged by one carboxylate ligand derived from the protein (Glu144), a hydroxide, and a water (or second hydroxo) molecule. It should be noted that the nature of the monodentate hydroxide bridging ligand in oxidized MMOH was inferred based on proton ENDOR studies on the mixed-valent [$Fe^{III}Fe^{II}$] form of the hydroxylase, which clearly showed the presence of a hydroxide bridge.[56,57] The Fe−O bond distances and Fe−O−Fe bond angles from the crystal structure are also consistent with this assignment. In addition to the bridging ligands, one Fe(III) ion (designated Fe2) is coordinated to one histidine (His246) and two monodentate carboxylate (Glu209 and Glu243) residues. The coordination sphere of the other Fe(III) ion (designated Fe1) is completed by one histidine (His147) residue, one monodentate carboxylate (Glu114) residue, and a terminal water molecule. The overall coordination environment of the binuclear iron center is generally consistent with ENDOR,[56−58] optical,[59] electron paramagnetic resonance (EPR),[37,39] extended

(30) Whittenbury, R.; Phillips, K. C.; Wilkinson, J. F. *J. Gen. Microbiol.* **1970**, *61*, 205.
(31) Higgins, I. J.; Best, D. J.; Hammond, R. C. *Nature* **1980**, *286*, 561.
(32) Fox, B. G.; Borneman, J. G.; Wackett, L. P.; Lipscomb, J. D. *Biochemistry* **1990**, *29*, 6419.
(33) Andersson, K. K.; Froland, W. A.; Lee, S.-K.; Lipscomb, J. D. *New J. Chem.* **1991**, *15*, 411.
(34) Colby, J.; Stirling, D. I.; Dalton, H. *Biochem. J.* **1977**, *165*, 395.
(35) Rataj, M. J.; Kauth, J. E.; Donnelly, M. I. *J. Biol. Chem.* **1991**, *266*, 18684.
(36) Green, J.; Dalton, H. *J. Biol. Chem.* **1989**, *264*, 17698.
(37) Fox, B. G.; Hendrich, M. P.; Surerus, K. K.; Andersson, K. K.; Froland, W. A.; Lipscomb, J. D.; Münck, E. *J. Am. Chem. Soc.* **1993**, *115*, 3688.
(38) Green, J.; Dalton, H. *J. Biol. Chem.* **1985**, *260*, 15795.
(39) Fox, B. G.; Froland, W. A.; Dege, J. E.; Lipscomb, J. D. *J. Biol. Chem.* **1989**, *264*, 10023.
(40) Lund, J.; Dalton, H. *Eur. J. Biochem.* **1985**, *147*, 291.
(41) Prince, R. C.; Patel, R. N. *FEBS Lett.* **1988**, *203*, 127.
(42) Froland, W. A.; Andersson, K. K.; Lee, S.-K.; Liu, Y.; Lipscomb, J. D. *J. Biol. Chem.* **1992**, *267*, 17588.
(43) Fox, B. G.; Liu, Y.; Dege, J. E.; Lipscomb, J. D. *J. Biol. Chem.* **1991**, *266*, 540.
(44) Liu, K.; Lippard, S. J. *J. Biol. Chem.* **1991**, *266*, 12836.
(45) Liu, K.; Lippard, S. J. *J. Biol. Chem.* **1991**, *266*, 24859.
(46) Paulsen, K. E.; Liu, Y.; Fox, B. G.; Lipscomb, J. D.; Münck, E.; Stankovich, M. T. *Biochemistry* **1994**, *33*, 713.
(47) Dalton, H. In *Applications of Enzyme Biotechnology*; Kelly, J. W., Ed.; Plenum Press: New York, 1991; p 55.
(48) Froland, W. A.; Dyer, D. H.; Radhakrishnan, R.; Earhart, C. A.; Lipscomb, J. D.; Ohlendorf, D. H. *J. Mol. Biol.* **1994**, *236*, 379.
(49) Nordlund, P.; Dalton, H.; Eklund, H. *FEBS Lett.* **1992**, *307*, 257.
(50) Stainthorpe, A. C.; Lees, V.; Salmond, G. P. C.; Dalton, H.; Murrell, J. C. *Gene* **1990**, *91*, 27.
(51) Liu, Y.; Nesheim, J. C.; Lee, S.-K.; Lipscomb, J. D. *J. Biol. Chem.* **1995**, *270*, 24662.
(52) Pulver, S.; Froland, W. A.; Fox, B. G.; Lipscomb, J. D.; Solomon, E. I. *J. Am. Chem. Soc.* **1993**, *115*, 12409.
(53) Rosenzweig, A. C.; Frederick, C. A.; Lippard, S. J.; Nordlund, P. *Nature* **1993**, *366*, 537.
(54) Rosenzweig, A. C.; Nordlund, P.; Takahara, P. M.; Frederick, C. A.; Lippard, S. J. *Chem. Biol.* **1995**, *2*, 409.
(55) The structure of the MMO from *M. trichosporium* OB3b has been determined at 2.0 Å for a crystal at room temperature. The structure of the active site cluster is essentially the same as the structure from MMOH from *M. capsulatus* shown in Figure 1A (Elango, N.; Radhakrishnan, R.; Froland, W. A.; Lipscomb, J. D.; Ohlendorf, D. H. Unpublished results). The structure of the *M. capsulatus* MMOH cluster at room temperature shows only a single μ-hydroxo bridge.[53]
(56) Thomann, H.; Bernardo, M.; McCormick, J. M.; Pulver, S.; Andersson, K. K.; Lipscomb, J. D.; Solomon, E. I. *J. Am. Chem. Soc.* **1993**, *115*, 8881.
(57) DeRose, V. J.; Liu, K. E.; Kurtz, D. M., Jr.; Hoffman, B. M.; Lippard, S. J. *J. Am. Chem. Soc.* **1993**, *115*, 6440.
(58) Hendrich, M. P.; Fox, B. G.; Andersson, K. K.; Debrunner, P. G.; Lipscomb, J. D. *J. Biol. Chem.* **1992**, *267*, 261.

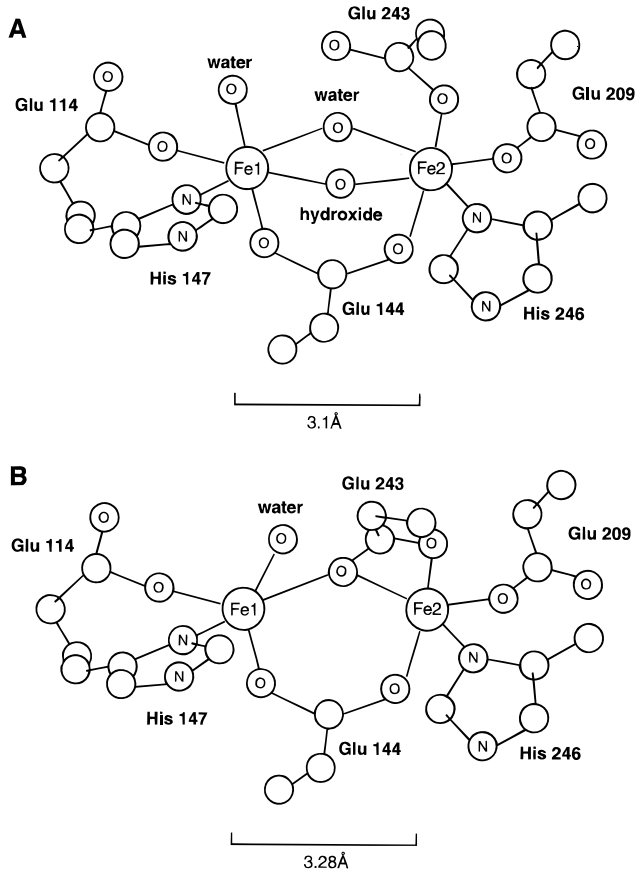

Figure 1. Schematic representation of the binuclear iron active site structure of the hydroxylase component of MMO from *Methylococcus capsulatus* (Bath): (A) oxidized MMOH; (B) reduced MMOH. Adapted from refs 53 and 54.

X-ray absorption fine structure (EXAFS),[60,61] and Mössbauer spectroscopic studies.[37,62] Recent EXAFS studies of MMOH from *M. trichosporium* OB3b show that the cluster in the resting enzyme is characterized by two populations with different Fe···Fe distances (3.0 and 3.4 Å).[61] Comparison with model studies suggests that these populations represent clusters with bis-μ-hydroxo and μ-hydroxo bridging ligands, respectively. These observations indicate that the structure of the cluster is flexible, which may be important for catalysis given the variety of intermediates that are found in the catalytic cycle.

The crystal structure of fully reduced MMOH, determined to 1.8 Å, reveals major differences in the coordination environment of the $Fe^{II}Fe^{II}$ center as compared to the binuclear ferric site of oxidized MMOH.[54] A schematic of the crystal structure is shown in Figure 1B. The Fe(II) atoms are no longer bridged by exogenous ligands, but by two protein derived glutamic acid residues (Glu144 and 243). It is important to note that Glu144 bridges in a μ-η^1,η^1 fashion, whereas Glu243 forms a μ-η^2 bridge and is also ligated in a bidentate manner to the ferrous atom designated Fe2. The coordination environment of Fe2 is completed by a histidine (His246) and a monodentate glutamic acid residue (Glu209). Similarly, Fe1 is coordinated to a histidine residue (His147), a monodentate glutamic acid residue (Glu114), and a terminal water molecule. As a result, both Fe(II) atoms are in a five-coordinate environment; however, the geometry at Fe2 is distorted due to the bidentate coordination mode of Glu243.

Circular dichroism (CD) and magnetic circular dichroism (MCD) spectroscopies provide direct probes of non-heme ferrous active sites,[63−67] since they allow the observation of ferrous d → d ligand field transitions which are weak in absorption and obscured by protein and buffer vibrations in the near infrared. Furthermore, variable-temperature variable-field MCD (VTVH MCD) on observed ligand field transitions can be used to estimate the zero field splitting (δ) and $g_{||}$ value of the ground state and the excited state sublevel energies of the dimer. These results can be further interpreted in terms of a spin Hamiltonian which includes the zero field splitting of each ferrous atom combined with the exchange coupling (J) between iron centers which reflects bridging ligation. CD and MCD studies on fully reduced MMOH have shown that the reduced hydroxylase site consists of two distorted five-coordinate Fe(II) ions with different geometries.[52] VTVH MCD studies demonstrated that the ground state has a $g_{eff} = 14.7$ which requires that the two ferrous ions be ferromagnetically coupled ($J \sim 0.3-0.5$ cm^{-1}), with each ion undergoing negative zero-field splitting to produce a $S_{Tot} = 4$, $M_S = \pm 4$ ground state. Small molecule binding studies on reduced MMOH have revealed that the CD spectrum remains unchanged upon the addition of anions, the enzymatic product, substrates, and inhibitor, suggesting that these molecules do not bind directly to the iron atoms or cause large perturbations in the iron site.[52] In contrast, dramatic changes in the CD and MCD spectra of MMOH upon addition of a ∼2-fold molar excess of MMOB are observed. However, the VTVH MCD and spin Hamiltonian parameters do not change significantly between MMOH and the MMOB complex. A ligand field analysis of the CD and MCD spectra showed that MMOB binding induces significant change in the geometry of only one Fe(II) ion, and it was suggested that the perturbed Fe(II) ion may play a role in the increased oxygen reactivity of the enzyme.[52]

In our earlier CD and MCD study on fully reduced MMOH, we used the spectral perturbations induced by MMOB to aid in the assignment of the ligand field bands in the reduced hydroxylase. Here we use CD and MCD studies of the Fe(II) ligand field transitions to investigate substrate, inhibitor, and small molecule binding to the binuclear non-heme ferrous center in the MMOH−MMOB complex in order to gain insight into the physiological mechanism of the enzyme.

Materials and Methods

All commercial reagents were used without further purification: D_2O (99.9 atom % D; Aldrich, Cambridge Isotope Laboratories), MOPS [3-(*N*-morpholino)propanesulfonic acid] (Sigma), d_3-glycerol (98 atom % D; Aldrich, Cambridge Isotope Laboratories), sodium dithionite (Aldrich), methyl viologen (Sigma), sodium azide (Aldrich), sodium chloride (Mallinckrodt), imidazole (Aldrich), methanol (Baker), *trans*-1,2-dichloroethylene (Aldrich), tetrachloroethylene (Baker), and methane (Liquid Carbonic).

MMOH and MMOB from *Methylosinus trichosporium* OB3b were purified and characterized according to published procedures.[39,68] The

(59) Andersson, K. K.; Elgren, T. E.; Que, L., Jr.; Lipscomb, J. D. *J. Am. Chem. Soc.* **1992**, *114*, 8711.
(60) DeWitt, J. G.; Bentsen, J. G.; Rosenzweig, A. C.; Hedman, B.; Green, J.; Pilkington, S.; Papaefthymiou, G. C.; Dalton, H.; Hodgson, K. O.; Lippard, S. J. *J. Am. Chem. Soc.* **1991**, *113*, 9219.
(61) Shu, L.; Liu, Y.; Lipscomb, J. D.; Que, L., Jr. *J. Biol. Inorg. Chem.* In press.
(62) Fox, B. G.; Surerus, K. K.; Münck, E.; Lipscomb, J. D. *J. Biol. Chem.* **1988**, *263*, 10553.
(63) Whittaker, J. W.; Solomon, E. I. *J. Am. Chem. Soc.* **1988**, *110*, 5329.
(64) Reem, R. C.; Solomon, E. I. *J. Am. Chem. Soc.* **1987**, *109*, 1216.
(65) Solomon, E. I.; Zhang, Y. *Acc. Chem. Res.* **1992**, *25*, 343.
(66) Solomon, E. I.; Kirk, M. L.; Gamelin, D. G.; Pulver, S. *Methods Enzymol.* **1995**, *246*, 71.
(67) Solomon, E. I.; Pavel, E. G.; Loeb, K. E.; Campochiaro, C. *Coord. Chem Rev.* **1995**, *144*, 369.
(68) Fox, B. G.; Froland, W. A.; Jollie, D. R.; Lipscomb, J. D. *Methods Enzymol.* **1990**, *188*, 191.

specific activities of the hydroxylase (4 mol Fe/mol hydroxylase) and component B were 1000−1200 and 10 000 nmol/min/mg, respectively. For NIR CD and MCD studies all MMOH and MMOB samples used were exchanged into 200 mM NaMOPS, 5% (^{1}H)glycerol, pD = 7.4 (99.9% D_2O). Concentrations were determined by absorbance at 282 nm, using ϵ_{282} = 539 mM^{-1} cm^{-1} per mol of hydroxylase and ϵ_{282} = 20.54 mM^{-1} cm^{-1} per mol of MMOB. Typically, 1.0−1.2 mM hydroxylase and 6.5−7.0 mM MMOB samples were prepared.

CD and MCD samples of the fully reduced MMOH were prepared by placing oxidized MMOH into a reaction vial. To this was added 100 μM of the redox mediator methyl viologen. The samples were made anaerobic by repeated cycles of evacuation and flushing with O_2-scrubbed nitrogen. Reduction was achieved by the anaerobic addition of excess sodium dithionite from a D_2O stock solution to the oxidized enzyme samples. The protein was allowed to incubate for approximately 15 min at room temperature and then transferred anaerobically to the appropriate sample holder. Samples of the reduced MMOH−MMOB complex were prepared by the addition of a 2−4-fold molar excess of anaerobic MMOB to reduced MMOH in the CD cell or reaction vial.

Small molecule binding studies were carried out in a cuvette previously sealed with a septum and deoxygenated. MMOH−MMOB−small molecule samples were prepared by the anaerobic addition of microliter quantities of a degassed solution of ligand in D_2O. The concentration of small molecules added was varied, up to a 250-fold molar excess. Changes were measured in the CD spectrum of the MMOH−MMOB complex upon the addition of microliter quantities of anaerobic solutions of substrate (15−25 mM for *trans*-1,2-dichloroethylene) or inhibitor (5 mM for tetrachloroethylene) to the reduced enzyme complex. Typically, an approximately 6-fold molar excess of substrate or inhibitor was used. The solubility of *trans*-1,2-dichloroethylene was determined at 23 °C in 0.2 M MOPS buffer, pD 7.6, through NMR proton integration using tetrahydrofuran as the reference, while a previously published value for the solubility of tetrachloroethylene was used.[32]

Near-IR CD spectra (600−2000 nm) were obtained on a Jasco 200D spectropolarimeter with an InSb detector. Samples were placed in a near infrared quartz cuvette and cooled to 5 °C by a recirculating water bath. Low-temperature CD and MCD spectra were obtained using the Jasco spectropolarimeter equipped with a modified sample compartment to accommodate an Oxford Instruments SM4−7T magnet/cryostat and focusing optics.[69] Final protein samples for low-temperature MCD experiments were in the form of a glass with 66% (v/v) degassed d_3-glycerol/0.2 M MOPS buffer plus 5% (^{1}H)glycerol at pD 7.4 in D_2O. Samples were injected anaerobically into an argon-purged MCD cell made by compressing a 2−3 mm rubber spacer between two infrasil quartz disks. Depolarization of the light by the MCD glass samples was monitored by their effect on the CD signal of a nickel (+)-tartrate solution placed before and after the sample.[70] In all cases, the depolarization was <10% at 4.2 K.

All MCD spectra presented were recorded between 4.2 and 5.0 K (unless otherwise noted) and 7.0 T with the natural CD (0.0 T) subtracted. CD spectra were obtained from samples in a 2 mm path length cuvette at 5 °C. The fits to the CD and MCD spectra were obtained with a Gaussian band shapes analysis using a constrained nonlinear least-squares fitting procedure.

Results and Analysis

A. Component B Binding to Fully Reduced MMOH. Figures 2A and 3A present the near-IR CD and low-temperature MCD spectra of reduced MMOH from 5500 (the D_2O cutoff) to 12 500 cm^{-1}. The CD spectrum shows two negative features at ∼10 000 and 7500 cm^{-1}, while the MCD spectrum shows two positive peaks at 7500 and 9000 cm^{-1} and one negative peak at ∼10 000 cm^{-1}. The CD and MCD spectra can be fit to three transitions at 7360 ± 100, 9140 ± 100, and 9900 ± 200 cm^{-1} with only the sign and intensity of the peaks changing between the spectra. Figure 2B shows the CD spectrum of the reduced MMOH in the presence of a 2−4-fold molar excess of MMOB relative to MMOH concentration (generally 1 mM MMOH). Figure 3B shows the corresponding low-temperature MCD spectrum. The addition of MMOB to reduced MMOH results in significant perturbation of the MMOH spectral features.

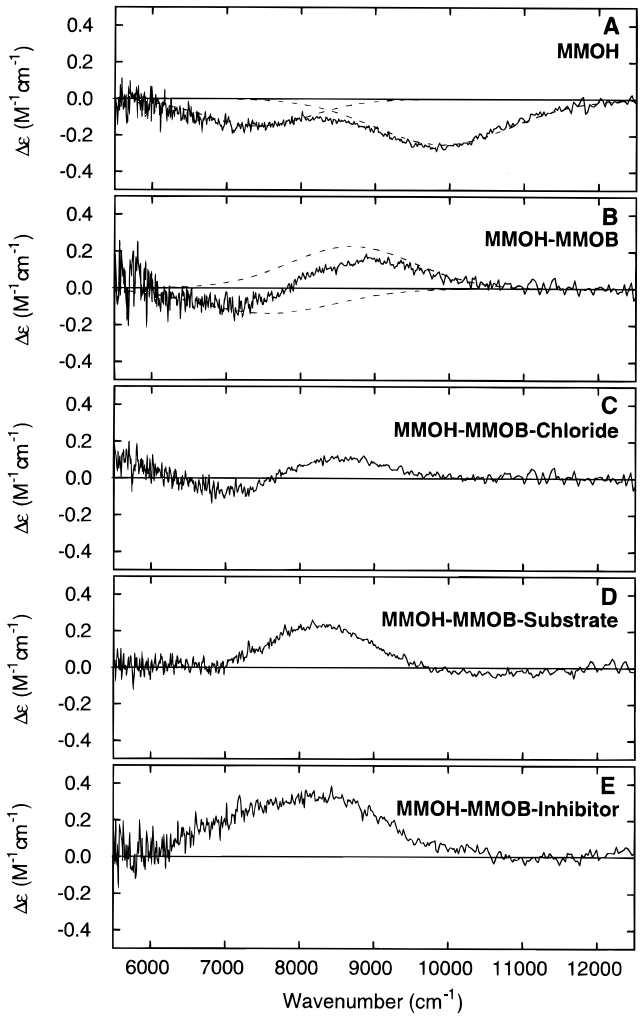

Figure 2. CD spectra of the binuclear non-heme Fe(II) active site in the fully reduced hydroxylase component of MMO: (A) reduced MMOH (dashed lines show the best fit Gaussian analysis of the data); (B) the MMOH−MMOB complex (dashed lines show the best Gaussian fit to the data); (C) the MMOH−MMOB complex with 50-fold molar excess sodium chloride; (D) the MMOH−MMOB complex with 3-fold molar excess *trans*-1,2-dichloroethylene; and (E) the MMOH−MMOB complex with 6-fold molar excess tetrachloroethylene. The CD spectra were recorded at 5 °C.

The MMOH−MMOB complex displays four transitions. Three positive bands are observed in the MCD spectrum which can be Gaussian resolved into a high energy feature at 9840 ± 100 cm^{-1} and two lower energy features at 7590 ± 100 and 6240 ± 100 cm^{-1}. The fourth band is only observed in the MMOH−MMOB CD spectrum and is located as a positive feature at 8650 ± 100 cm^{-1}. The energies and band shapes of the transitions observed in the CD spectrum are unaffected by the addition of the glassing agent glycerol. Ligand field transitions observed in CD and MCD for MMOH and the MMOH−MMOB complex are summarized in Table 1. Comparison between the CD and MCD spectra of MMOH and the MMOH−MMOB complex shows that the MMOH−MMOB

(69) Spira-Solomon, D. J.; Allendorf, M. D.; Solomon, E. I. *J. Am. Chem. Soc.* **1986**, *108*, 5318.

(70) Browett, W. R.; Fucaloro, A. F.; Morgan, T. V.; Stephens, P. J. *J. Am. Chem. Soc.* **1983**, *105*, 1868.

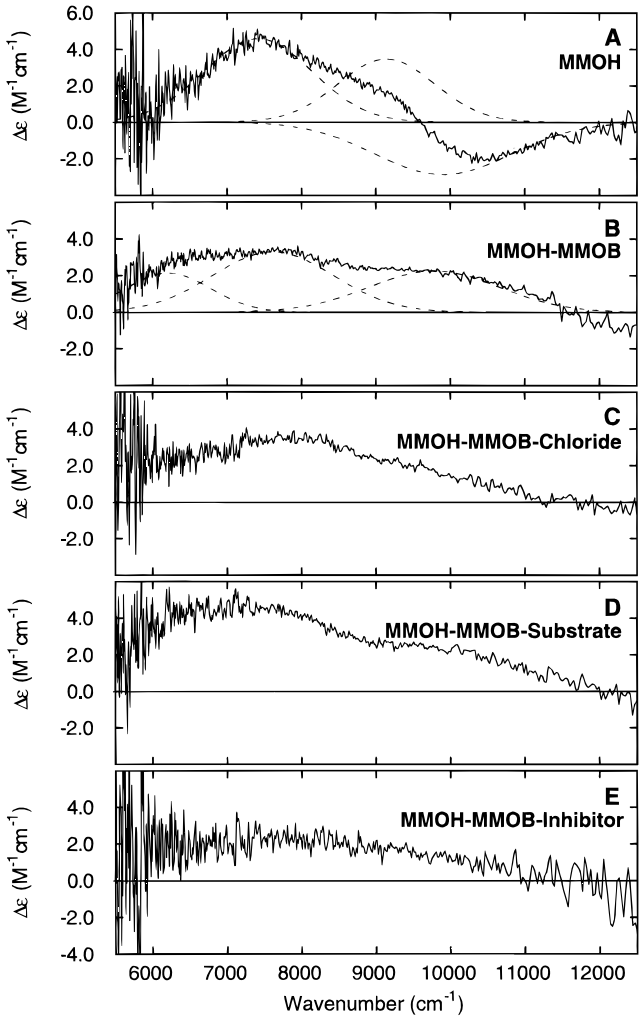

Figure 3. MCD spectra of the binuclear non-heme Fe(II) active site in the fully reduced hydroxylase component of MMO: (A) reduced MMOH (dashed lines show the best fit analysis of the data); (B) the MMOH−MMOB complex (dashed lines show the best Gaussian fit to the data); (C) the MMOH−MMOB complex with 50-fold molar excess sodium chloride; (D) the MMOH−MMOB complex with 3-fold molar excess *trans*-1,2-dichloroethylene; and (E) the MMOH−MMOB complex with ~6-fold molar excess tetrachloroethylene. The MCD spectra were recorded at 4.2−5 K and 7.0 T.

spectrum has three bands at approximately the same energy as MMOH and one additional low-energy feature.

Both reduced MMOH and the MMOH−MMOB complex have greater than two d → d transitions, indicating that the iron atoms are inequivalent. A high-spin d^6 Fe(II) ion in an octahedral field exhibits two MCD bands between 8000 and 12 000 cm^{-1} for predominantly oxygen and nitrogen ligation. In five-coordinate geometries, the ligand field bands are split to a greater extent ($\Delta E \sim 5000$ cm^{-1}) and lie at approximately 5000 and 10 000 cm^{-1}. For tetrahedral four coordinate sites, the spin allowed ligand field transitions will occur in the region of 4000 to 6500 cm^{-1}. Both MMOH and the MMOH−MMOB complex show transitions below 8000 cm^{-1}, which is consistent with lower than six-coordinate environments. Based on the number and location of the ligand field transitions, it was proposed that the ferrous atoms in the active site of reduced MMOH and MMOH−MMOB are both five coordinate with different geometries. A detailed analysis of the ligand field features observed in reduced MMOH and the MMOH−MMOB complex is presented in ref 52.

B. Small Molecule Binding to the MMOH−MMOB Complex. The effect of exogenous ligand binding to the binuclear ferrous active site of the MMOH−MMOB complex was probed by titrating different concentrations of exogenous ligand into the reduced enzyme complex and monitoring the CD spectrum. The CD spectrum of the fully reduced MMOH−MMOB complex remained unchanged upon anaerobic addition of the small molecules N_3^- and Cl^-, and the enzymatic product methanol. The concentration of small molecules added to the MMOH−MMOB complex in the CD cell was varied up to a 250-fold molar excess relative to protein (0.7 mM MMOH). Figure 2C presents the CD spectrum of the MMOH−MMOB complex plus 50-fold molar equiv of chloride; it is essentially unchanged from the MMOH−MMOB spectrum (Figure 2B). Based on our ability to detect changes in the CD spectra, we estimate that the K_B values for Cl^-, N_3^-, and methanol must be <18, 7, and 30 M^{-1}, respectively.

Figure 3C presents the MCD spectrum associated with the MMOH−MMOB plus chloride system. As in the CD spectrum, addition of chloride does not significantly perturb the MCD spectrum of the MMOH−MMOB complex (Figure 3B). Gaussian fitting of the MMOH−MMOB−Cl spectrum results in the identification of three positive peaks located at 9830 ± 100, 7810 ± 150, and 6020 ± 100 cm^{-1}. These features correspond well to the ligand field transitions observed in the MMOB complex: 9840 ± 100, 7590 ± 100, and 6240 ± 100 cm^{-1}. MCD Gaussian best fit data are summarized in Table 1. The results described here suggest that azide, chloride, and methanol do not bind to the iron atoms in the MMOH−MMOB complex. This observation parallels the results of studies on the reduced hydroxylase in the absence of MMOB where no spectral perturbation is observed.[52]

C. Substrate and Inhibitor Binding to the MMOH−MMOB Complex. Substrate and inhibitor effects on the binuclear iron active site of the MMOH−MMOB complex were also studied. We have previously shown that *trans*-1,2-dichloroethylene (CHCl═CHCl) is a substrate with comparable turnover number and K_M values to methane, but with a much higher solubility as required to conduct CD/MCD experiments near the solubility limit of the proteins.[32] Similarly, it was shown that tetrachloroethylene (CCl_2═CCl_2) is a competitive inhibitor for the enzyme with a K_I value of 90 μM. Significant changes are observed in the CD spectrum following the anaerobic addition of a 3-fold molar excess of *trans*-1,2-dichloroethylene and a 6-fold excess of tetrachloroethylene to the reduced complex (Figures 2D and 2E, respectively). In Figure 2D, the negative ~7300 cm^{-1} d → d excited-state feature observed in the MMOH−MMOB sample (Figure 2B) has decreased in intensity as it is no longer visible in the substrate−bound enzyme complex. In addition, upon anaerobic substrate binding, the positive CD feature at ~8600 cm^{-1} in the MMOH−MMOB complex is shifted to somewhat lower energy (ΔE = 200 cm^{-1}) and has increased in intensity by ~25%. The CD band increases in intensity with the addition of up to a 3-fold molar excess CHCl═CHCl with respect to MMOH concentration. Further addition of substrate produces no additional change, indicating that the substrate binding is saturated. Gaussian fitting of the MMOH−MMOB−substrate spectrum requires only one peak at 8450 ± 100 cm^{-1}.

Inhibitor (tetrachloroethylene) binding results in similar perturbations of the CD spectrum of the ferrous active site of the MMOH−MMOB complex. As shown in Figure 2E, the negative band observed at 7300 cm^{-1} in the MMOH−MMOB complex exhibits the opposite sign in the inhibitor bound sample. Furthermore, the band at ~8480 cm^{-1} has shifted to lower energy and increased in intensity by ~70% relative to the related feature in uncomplexed MMOH−MMOB. Gaussian fitting

Table 1. CD and MCD Gaussian Fitting Results for Reduced MMOH, the Reduced MMOH−MMOB Complex, and the MMOH−MMOB−Ligand Complexes

		reduced MMOH		MMOH−MMOB		MMOH−MMOB−Cl		MMOH−MMOB−substrate		MMOH−MMOB−inhibitor	
band		CD	MCD	CD	MCD	CD	MCD	CD	MCD	CD	MCD
1[a]	energy (cm^{-1})[b]				(+)[d] 6170		(+) 6020		(+) 6165		(+) 5940
	hwhm (cm^{-1})[c]				680		1300		940		1000
2	energy (cm^{-1})	(−) 7360	(+) 7360	(−) 7330	(+) 7590	(−) 7320	(+) 7810	(+) 8450	(+) 7820	(+) 7240	(+) 7830
	hwhm (cm^{-1})	1090	1090	800	1280	800	1230	930	1100	800	1150
3	energy (cm^{-1})	(−) 9140	(+) 9140	(+) 8650		(+) 8385				(+) 8470	
	hwhm (cm^{-1})	945	940	910		990				930	
4	energy (cm^{-1})	(−) 9900	(−) 9900		(+) 9840		(+) 9840		(+) 9900		(+) 9650
	hwhm (cm^{-1})	1300	1300		1100		1240		1300		1300

[a] These values should be regarded as estimates, since the band position is at the limit of the spectrometer thus the data are relatively noisy. [b] Energies are accurate within ±200 cm^{-1}. [c] Half widths at half maximum height are accurate within ±200 cm^{-1}. [d] Indication of the sign of the CD/MCD ligand field transitions.

results of both the substrate- and inhibitor-bound forms of the MMOH−MMOB complex are presented in Table 1. Comparison of the MMOH−MMOB complex CD spectrum (Figure 2B) with Figures 2D and 2E clearly shows that the MMOH−MMOB−CHCl═CHCl (or CCl_2═CCl_2) spectrum is not the same as the resting MMOH−MMOB spectrum, demonstrating that, in contrast to the lack of an effect in the resting protein,[52] the addition of substrate (or inhibitor) perturbs the binuclear ferrous site when MMOB is bound.

Figure 3D gives the low-temperature MCD spectrum of the MMOH−MMOB−substrate complex. The spectrum displays a number of overlapping transitions in the region from 5500 to 10 000 cm^{-1} that can be resolved into a minimum of three positive d → d transitions at 9897, 7820, and 6165 cm^{-1}. In contrast to the significant effects observed in the CD spectra upon substrate binding, the MCD spectrum of the MMOH−MMOB complex (Figure 3B) remains largely unchanged upon anaerobic addition of *trans*-1,2-dichloroethylene. The low-temperature MCD spectrum of the MMOH−MMOB complex remains similarly unchanged in the presence of the inhibitor tetrachloroethylene (Figure 3E). Due to the low solubility of CCl_2═CCl_2 in buffer, a relatively large volume of inhibitor had to be added to the MMOH−MMOB complex to ensure saturating conditions ($K_i \sim 90\ \mu M$). As a result, the MCD spectrum of the inhibitor bound complex has a lower signal to noise ratio than the other MCD spectra presented in Figure 3. Gaussian spectral resolution of Figure 3E gives three transitions at ∼9650, 7800, and 6000 cm^{-1} (Table 1).

D. Small Molecule Binding to the MMOH−MMOB−Substrate Complex. Azide titration studies were carried out on the MMOH−MMOB-substrate complex, to determine if substrate binding activates MMOH for small molecule binding. The CD spectrum of the substrate-bound MMOH−MMOB complex remained unchanged even up to a 60-fold molar excess of azide ($K_B < 7\ M^{-1}$). This parallels the behavior of MMOH and the MMOH−MMOB complex in that the binuclear ferrous active site in MMOH does not bind anions.

E. Saturation Magnetization. The MCD data presented in Figure 3 increase in signal intensity as temperature decreases indicating that these transitions are MCD C-terms. Thus the ground state of fully reduced MMOH, the MMOH−MMOB complex, and the MMOH−MMOB−substrate and inhibitor complexes are paramagnetic doublets which split in energy in a magnetic field. The field saturation curves measured on the positive band at 1290 nm (7750 cm^{-1}) for MMOH−MMOB and MMOH−MMOB−CHCl═CHCl are plotted as a function of the reduced parameter $\beta H/2kT$ for a series of fixed temperatures in Figure 4 (parts A and B, respectively). These isotherms do not superimpose; i.e. they show a nested behavior, resulting

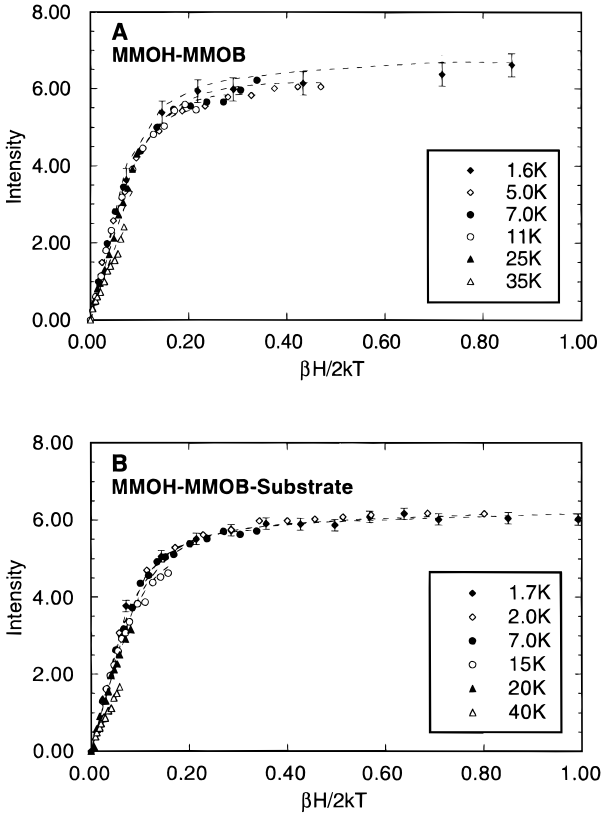

Figure 4. Saturation−magnetization behavior for (A) the MMOH−MMOB complex at 1290 nm (7750 cm^{-1}) and (B) the MMOH−MMOB−*trans*-1,2-dichloroethylene complex at 1290 nm (7750 cm^{-1}). The MCD intensity amplitude for a range of magnetic fields (0−7.0 T) at a series of fixed temperatures is plotted as a function of $\beta H/2kT$. The fit to the VTVH MCD data (--) was obtained by substituting the parameters presented in the text into eq 1 in ref 52. The error bars for the lowest temperature points have been included and are representative of the error for all the data points.

from zero-field splitting (ZFS) of the paramagnetic ground state.[65,67,71] Such behavior is generally observed for systems with an integer spin (non-Kramers) ground state. In addition to the nesting behavior, the saturation−magnetization curves increase linearly with increasing field at lowest temperature and high fields. A pure C-term will saturate at low temperature and high field, therefore this reflects an additional contribution from linear field induced mixing with higher-lying excited states (i.e. a MCD B-term). The saturation−magnetization MCD behavior can be fit using a non-Kramers doublet model, to quantitatively determine the ground state parameters $g_{||}$ and δ

(71) Thomson, A. J.; Johnson, M. K. *Biochem. J.* **1980**, *191*, 411.

(the magnitude of the ZFS of the non-Kramers doublet ground state) as well as the position of low-lying excited states.[63,67,72]

As described in our previous study,[52] iterative fitting of the VTVH MCD data of the MMOH−MMOB complex gave a ground state best fit of $g_{||} = 16.2 \pm 0.6$ and $\delta < 1.0$ cm^{-1} with a small B-term contribution of ∼1%. In addition, low-lying excited states were required to accurately describe the high-temperature data. Fitting of the saturation−magnetization data of the MMOH−MMOB−substrate complex to eq 1 in ref 52 yields the ground state parameters $g_{||} = 16.1 \pm 0.5$ and $\delta < 1.0$ cm^{-1} with a B-term contribution of ∼0.6%. These parameters correlate well with those of the MMOH−MMOB complex. In addition, as was the case with MMOH−MMOB, excited states at ∼5 and 12 cm^{-1} must be included in order to obtain good fits to the complete VTVH data range. The saturation−magnetization behavior of the MMOH−MMOB complex in the presence of Cl^-, N_3^-, MeOH, and $CCl_2{=}CCl_2$ can also be fit using the parameters for the uncomplexed MMOH−MMOB sample.

Discussion

A. Effect of MMOB on Substrate Interactions with MMOH. Spectroscopic studies on the fully reduced form of MMOH revealed that substrates, products, inhibitors, and anionic small molecules do not perturb the binuclear ferrous active site.[52] It is likely that the substrates and inhibitors bind in the MMOH−substrate site at some point in the catalytic cycle, but the lack of significant spectral perturbation suggests that direct binding to the iron in the biferrous cluster is not involved. There are several indications that MMOB changes the MMOH active site conformation. For example, addition of MMOB to the reduced hydroxylase caused the $g = 16$ EPR signal associated with the coupled binuclear ferrous site to become sharper and more intense.[73] Also, CD and MCD studies revealed that the ligand field of one iron atom in the [$Fe^{II}Fe^{II}$] active site is significantly perturbed when MMOB binds to MMOH.[52] In the present study, the effects of small molecule, substrate, and inhibitor binding to the binuclear ferrous active site in the MMOH−MMOB complex of methane monooxygenase were probed. Our results show significant changes in the CD spectrum of the MMOH−MMOB complex in the presence of a ∼3-fold molar excess of the substrate, *trans*-1,2-dichloroethylene, and a ∼6-fold molar excess of the inhibitor, tetrachloroethylene (Figure 2). *These suggest that the formation of the MMOH−MMOB complex changes the conformation of the binuclear ferrous active site, such that substrate interacts more strongly with the binuclear metal center than in uncomplexed MMOH. This is the first indication of this effect of MMOB.*

The CD results also correlate well with the rate enhancement observed in the enzymatic reaction upon MMOB binding, which can be as much as 150 fold in initial velocity for some substrates.[43] Recently, we have shown that the major cause of this rate enhancement is a 1000 fold (at 4 °C) increase in the rate of oxygen reaction with the biferrous MMOH−MMOB complex relative to the rate with the uncomplexed biferrous MMOH.[51] Also, the rate of spontaneous conversion of the resulting peroxy complex, compound P, to form the hydrocarbon reactive complex, compound Q, is increased about 40 fold. Together these rate increases shift the rate limiting step for turnover to product release. Although the chemical basis for the rate enhancement has not been established, it appears to be correlated with an increase in the accessibility of the binuclear cluster to O_2. This is consistent with a change in the local or global protein conformation as revealed here by the changes in substrate interaction with the cluster which are only observed in the presence of MMOB.

Another indication of the effects of MMOB on MMOH structure has come through the observation that the product distribution of substrates more complex than methane is altered by formation of the MMOH−MMOB complex.[42] In the case of isopentane oxidation, hydroxylation occurs preferentially at the lowest energy (tertiary) carbon−hydrogen bond in the absence of MMOB, while in its presence the distribution shifts to a preference for the primary carbon hydroxylation. We proposed that the shift is reflective of a conformational change that alters the way in which the substrate can physically approach the binuclear iron cluster. The present results support such a change in the active site.

B. Assignment of Ligand Field Bands to Specific Iron Atoms in the Cluster. The spectral perturbations induced by MMOB on the reduced MMOH, and the changes observed in the MMOH−MMOB complex in the presence of substrate and inhibitor, allow for a probable assignment of the ligand field bands. The MCD spectrum of reduced MMOH shows two positive d → d transitions at ∼7400 and 9100 cm^{-1}, and one negative transition at 9900 cm^{-1} (Figure 3A). The reduced MMOH−MMOB complex shows four ligand field transitions at ∼6200, 7500, 8600, and 9800 cm^{-1} (Table 1). Thus MMOB perturbs the hydroxylase MCD spectrum most dramatically by raising the energy of an unobserved low-energy band and by changing the MCD sign of the feature at ∼9900 cm^{-1} (Figures 3A and 3B). These MCD spectral changes indicate that one five-coordinate Fe(II) atom is associated with the transitions at ∼7500 and 8600 cm^{-1} that are least affected, while the significantly altered features at ∼6200 and 9800 cm^{-1} correspond to the other five-coordinate ferrous center in the MMOH−MMOB complex. It should also be noted that the negative 9100-cm^{-1} band observed in the CD spectrum of reduced MMOH has changed sign upon MMOB binding (Figures 2A and 2B). While MCD spectral changes reflect differences in the electronic structure of the binuclear iron center, CD is sensitive to changes in the general protein environment in the vicinity of the iron center. Therefore, the CD and MCD spectral changes arising from MMOB binding suggest that MMOB affects both Fe(II) atoms in the active site, but one more directly.

Comparison of the CD spectrum of the MMOH−MMOB complex (Figure 2B) with those of the MMOH−MMOB−substrate and MMOH−MMOB−inhibitor complexes (Figures 2D and 2E, respectively), provide further insight into active site changes. Both *trans*-1,2-dichloroethylene and tetrachloroethylene perturb the 8600- and 7500-cm^{-1} bands of the MMOH−MMOB complex. In the case of *trans*-1,2-dichloroethylene, the 7500-cm^{-1} band has greatly decreased in intensity, while the 8600-cm^{-1} band has gained intensity. For tetrachloroethylene, the 8600-cm^{-1} feature also gains intensity, but the negative low-energy feature changes sign upon inhibitor binding. Corresponding changes in the MCD spectra of these complexes (Figure 3B,D,E) are not observed, indicating that substrate and inhibitor perturb the active site pocket but not the binuclear ferrous center (i.e. these do not directly coordinate to the Fe(II)). Furthermore, the two CD transitions affected by substrate binding are not the bands perturbed by MMOB binding to the reduced hydroxylase (9800 and <5000 cm^{-1}, *vide supra*). *These observations suggest that MMOB changes the ligand field*

(72) McCormick, J. M. Ph.D. Thesis, Stanford University, 1991.
(73) Hendrich, M. P.; Münck, E.; Fox, B. G.; Lipscomb, J. D. *J. Am. Chem. Soc.* **1990**, *112*, 5861.

environment significantly at one Fe(II) atom of the binuclear ferrous center, while substrate binding perturbs the other Fe(II) atom.

These spectral observations correlate well to the crystal structure of MMOH.[53,54] The crystal structure indicates that there is no direct access from the surface of the protein to the active center. Therefore the binding of substrate might be influenced by any event that changes the resting structure so that substrates have more access to the cluster, such as that proposed here for the MMOB interaction. Based on the crystal structure of MMOH, it has been suggested that a possible binding site for MMOB is located at the interface of the α and β subunits.[53] This putative binding site is in close proximity to the amino acid residues Glu209, Glu243, and His246, all of which are coordinated to Fe2 in the crystal structure (Figure 1).[54] Providing that MMOB actually binds near these residues, and based on the CD and MCD results discussed above and in greater detail in ref 52, we would correlate the ligand field transitions at 9800 and ~6200 cm^{-1} in the MCD spectrum of the MMOH−MMOB complex to Fe2 (Figure 3B). The transitions at 7500 and ~8600 cm^{-1} will, therefore, be associated with Fe1, and the substrate and inhibitor binding site would appear to be in closer proximity to this Fe(II) center (*vide supra*).

C. Ligand Field Calculations. The d → d transitions observed here probe the ligand field at the individual Fe(II) centers. Approximate ligand field calculations[74] were performed on a model of the reduced MMOH site that was generated from the coordinates of the oxidized structure which were adjusted based on the superposition of the oxidized and reduced MMOH structures shown in Figure 5 of ref 54 and described in the introduction.[75] It is important to note that while both iron atoms become five-coordinate on reduction, Fe1 has a square-pyramidal geometry with four short O bonds and one long equatorial N bond, while Fe2 is in a more distorted environment owing to the bidentate coordination mode of Glu243 and has four long O bonds and one short N bond.[54]

Ligand field calculations were performed by adjusting the relative strength of the ligands surrounding each Fe(II) atom according to ligand type (N or O) and bond length.[76] These calculations predict the ^5E_g excited state splitting of Fe1 to be smaller than the corresponding splitting in Fe2. Extending this observation to the experimentally observed ligand field transitions in reduced MMOH (Figures 2A and 3A) suggests that the bands at ~7500 and 9100 cm^{-1} ($\Delta^5E_g = \sim 1600$ cm^{-1}) are associated with Fe1, while the bands at <5000 and 9900 cm^{-1} ($\Delta^5E_g > 4900$ cm^{-1}) correspond to Fe2. Therefore, the correlation of the d → d transitions to the ligand fields of specific Fe(II) centers is in agreement with the MMOB and substrate perturbation assignment described above which was based on crystallographic results.

D. Correlation with Other Proteins Containing Binuclear Iron Centers. A binuclear iron center similar to that found in methane monooxygenase is also present in hemerythrin[77,78] and in the R2 subunit of ribonucleoside diphosphate reductase.[79] Spectroscopic and crystallographic studies have established that the binuclear ferrous center of hemerythrin (deoxyHr) has one six- and one five-coordinate ferrous atom.[77] CD and MCD studies suggest that the active site of reduced R2 consists of one five- and one four-coordinate Fe(II).[80,81] Therefore, the reduced sites in MMOH, Hr and R2 are all coordinatively unsaturated, leading to the possibility of small molecule binding. Azide binding studies demonstrated that this ligand binds to the open coordination position on the five-coordinate Fe(II) of deoxyHr ($K_B = 70$ M^{-1}), resulting in two six-coordinate Fe(II) ions.[64] Azide titration studies on fully reduced R2 indicate that exogenous ligand binding also occurs in RDPR but with a reduced affinity ($K_B \sim 21$ M^{-1}).[81,82] In contrast, azide and other anionic ligands do not bind to the binuclear ferrous center in MMOH even in the presence of MMOB and substrate ($K_B < 7$ M^{-1}).

Insight into the different small molecule binding reactivities of deoxyHr and reduced R2 RDPR and MMOH can be gained from the coordination environment of the binuclear ferrous active site in these proteins. The crystal structure of deoxyHr shows that the Fe(II) atoms are bridged by two carboxylate residues and an exogenous hydroxide ligand.[77] The coordination environment of one Fe(II) atom is completed by three histidine residues, and the other Fe(II) atom is ligated to two histidine residues. Since histidines are neutral ligands, the $Fe^{II}Fe^{II}$ center has an overall positive charge. Therefore anionic small molecules interact well with the active site. In contrast, the biferrous center of reduced RDPR consists of one four- and one five-coordinate Fe(II) atom which are bridged by two carboxylate residues.[81,83,84] The coordination environment for the four-coordinate center is completed by one carboxylate and one histidine residue, while the five-coordinate center is ligated to a carboxylate, a histidine, and either a terminal water or a second oxygen from the carboxylate ligand. The abundance of carboxylate ligands in the active site of reduced R2, as compared to deoxyHr, leads to a neutral biferrous center with stronger donor ligation, which is reflected in the decrease of K_B for small anion binding to reduced R2.

The active site cluster of reduced MMOH is fairly similar to that of reduced R2; however, small molecules do not bind to the biferrous cluster of MMOH. The primary differences between the two $Fe^{II}Fe^{II}$ centers are that both Fe(II) atoms in MMOH are five-coordinate, and that one carboxylate residue bridges in a μ-η^2 fashion and is also ligated in a bidentate manner to one of the Fe(II) atoms. As a result of the μ-η^2 bridging mode, the Fe···Fe distance is ~3.3 Å in reduced MMOH[54] which is significantly shorter than the corresponding distance of 3.8 Å observed in reduced R2.[84] The more compact nature of the biferrous active site in MMOH and the increase in coordination number at the active site could provide enough steric hindrance and charge donation such that small anionic molecules cannot bind to fully reduced MMOH. Alternatively, the environment of the cluster in MMOH may also inhibit anion binding. Indeed, long solvent interactions are present to each open coordination site on the cluster irons which may inhibit anion binding either sterically or by giving the ensemble a partial negative charge if the solvents are extensively hydrogen bonded.

(74) Companion, A. L.; Komarynsky, M. A. *J. Chem. Educ.* **1964**, *41*, 257.

(75) Only the crystallographic coordinates of oxidized MMOH are presently available from the Brookhaven protein data bank.

(76) Initial estimates of the ligand field parameters (α_2, α_4) (cm^{-1}) were based on model complexes as described in ref 52. Final parameters (cm^{-1}) used in the ligand field calculations are the following: Fe1: N-His_{147} (12000, 1500), O-Glu_{114}, -H_2O (13700, 1900), O-Glu_{144}, -Glu_{243} (12000, 1300); Fe2: N-His_{246} (22250, 7000), O-$Glu_{243\ OE2}$, -$Glu_{243\ OE1}$, -Glu_{144} (9500, 500), O-Glu_{209} (10900, 800).

(77) Holmes, M. A.; Trong, I. L.; Turley, S.; Sieker, L. C.; Stenkamp, R. E. *J. Mol. Biol.* **1991**, *218*, 583.

(78) Holmes, M. A.; Stenkamp, R. E. *J. Mol. Biol.* **1991**, *220*, 723.

(79) Nordlund, P.; Sjöberg, B.-M.; Eklund, H. *Nature* **1990**, *45*, 593.

(80) McCormick, J. M.; Reem, R. C.; Foroughi, J.; Bollinger, J. M.; Jensen, G. M.; Stephens, P. J.; Stubbe, J.; Solomon, E. I. *New J. Chem.* **1991**, *6*, 439.

(81) Pulver, S. C.; Tong, W. H.; Bollinger, J. M.; Stubbe, J.; Solomon, E. I. *J. Am. Chem. Soc.* **1995**, *117*, 12664.

(82) Elgren, T. E.; Hendrich, M. P.; Que, L., Jr. *J. Am. Chem. Soc.* **1993**, *115*, 9291.

(83) Atta, M.; Nordlund, P.; Åberg, A.; Eklund, H.; Fontecave, M. *J. Biol. Chem.* **1992**, *267*, 20682.

(84) Åberg, A. Ph.D. Thesis, Stockholm University, 1993.

The increase in negative charge at the MMOH active site is also manifested in the $Fe^{III}Fe^{III}$ oxidation state, by the presence of a hydroxide[54,56,57] bridging ligand rather than the μ-oxo bridge present in oxy- and metHr[77,78] and the oxidized R2 subunit of RDPR.[11,79]

The differences in charge donation in the binuclear ferrous active sites of MMOH, the R2 subunit of RDPR, and deoxyHr appear to correlate with the differences in O_2 reactivity displayed by these enzymes. In MMOH, the reaction of the binuclear ferrous site with O_2 produces a ferric-peroxy-bound intermediate[85] which undergoes heterolytic O−O bond cleavage to produce water and a comparatively long-lived $[Fe^{IV}Fe^{IV}]$═O intermediate (compound Q).[3,85,86] The strong donor ligation of the MMOH active site may enhance the formation and stability of this ferryl intermediate. In the case of RDPR, dioxygen activation results in the formation of a semistable intermediate which is best described as having an $[Fe^{III}Fe^{IV}]$ cluster with considerable charge delocalization onto the bridging oxygens (intermediate X).[87−89] This intermediate is one-electron reduced from compound Q. If a species equivalent to compound Q also occurs in RDPR, it must be short lived as it is not detected. It is not known at present why this is the case, but it may relate to rapid reduction by an exogenous donor, rapid hydrogen atom abstraction from a nearby amino acid, or insufficient electron density in the site to stabilize this highly electron deficient species. The latter explanation would be in accord with the finding reported here for MMOH but the others are equally plausible. Reversible dioxygen binding to deoxyHr results in the formation of a biferric center which has a peroxide bound to one ion in an end-on fashion (oxyHr).[23−25] The abundance of histidine ligands in Hr results in a more positive less electron donating site, stabilizing oxyHr toward further activation of the peroxide.

Conclusions

In summary, the results of the CD and MCD analysis have provided insight into substrate and exogenous ligand interactions with the binuclear ferrous active site of the MMOH−MMOB complex of methane monooxygenase. It has been found that substrate and inhibitor binding induce a conformational change in the active site pocket of the MMOH−MMOB complex but do not directly affect the coordination environment of the binuclear iron center. Furthermore, these changes differ from the perturbations caused by MMOB binding to the reduced MMOH. As a result, the spectral features of each ferrous atom can be distinguished and correlated with the crystal structure of MMOH. Small molecule binding studies reveal that the biferrous center of reduced MMOH is not effective in anionic ligand binding, which is a reflection of the less electrophilic nature of the reduced MMOH active site due to the presence of strong donor ligation. Comparison of the site in MMOH, RDPR, and Hr indicates that differences in relative charge donation of the binuclear iron active sites provide one important correlation with their differences in dioxygen reactivities.

Investigations of the transient kinetics of the reactions of the intermediates in the catalytic cycle of MMOH have shown that the first species to be kinetically affected by substrates is compound Q.[86] Moreover, substrates react with compound Q in what appears kinetically as a second-order reaction, probably indicating a very short lived enzyme complex before catalysis occurs. Consequently, the findings reported here that indicate substrates can perturb the binuclear ferrous cluster probably do not mean that the substrate binds in the active site in a mechanistically significant manner prior to oxygen activation. Nevertheless, it is unlikely that large structural changes occur during the rapid formation of compound Q following the reaction of the biferrous cluster with O_2. Thus, the structural insight regarding the interaction of the substrate with the cluster is likely to apply also to the interaction with compound Q. This is the first such insight to be gained from any investigation of this enzyme.

Acknowledgment. This work was supported by NSF-Biophysics Program Grant MCB 9316768 (E.I.S.) and NIH Grant GM 40466 (J.D.L.).

JA962854I

(85) Liu, K. E.; Wang, D.; Huynh, B. H.; Edmondson, D. E.; Salifoglou, A.; Lippard, S. J. *J. Am. Chem. Soc.* **1994**, *116*, 7465.
(86) Lee, S.-K.; Nesheim, J. K.; Lipscomb, J. D. *J. Biol. Chem.* **1993**, *268*, 21569.
(87) Ravi, N.; Bollinger, J. M.; Huynh, B. H.; Edmondson, D. E.; Stubbe, J. *J. Am. Chem. Soc.* **1994**, *116*, 8007.
(88) Ravi, N.; Bominaar, E. L. *Inorg. Chem.* **1995**, *34*, 1040.
(89) Sturgeon, B. E.; Burdi, D.; Chen, S.; Huynh, B.-H.; Edmondson, D. E.; Stubbe, J.; Hoffman, B. M. *J. Am. Chem. Soc.* **1996**, *118*, 7551.